Low Cost Dual Rotating Infrared Sensor for Mobile Robot Swarm Applications

post IROS2009 paper

***Abstract*—This paper presents a novel low-cost position detection prototype from practical design to implementation of its control schemes. This prototype is designed to provide mobile robot swarms with advanced sensing capabilities in an efficient, cost-effective way. From the observation of bats' foraging behaviors, the prototype with a particular emphasis on variable rotation range and speed, as well as 360-degree observation capability has been developed. The prototype also aims at giving each robot reliable information about identification of neighboring robots from objects and their positions. For this purpose, an observation algorithm-based sensor is proposed. The implementation details are explained, and the effectiveness of the control schemes is verified through extensive experiments. The sensor provides real-time location of stationary targets positioned 100 cm away within an average error of 2.6 cm. Moreover, experimental results show that the prototype observation capability can be quite satisfactory for practical use of mobile robot swarms.**

***Index Terms*—proximity sensor, 360-degree observation, target tracking, cost-effectiveness, mobile robot swarm**

I. INTRODUCTION

WITH recent advances in robotics, much attention has been paid to the use of mobile robot swarms. They offer many advantages in terms of efficiency, fault-tolerance, adaptability, and so on [1]. To achieve and maintain such capabilities, decentralized coordination approaches controlling the motions of individual robots have been reported, such as pattern generation [2][3], self-configuration [4][5], and flocking [6][7]. These enable large-scale robot swarms to successfully perform many potential applications: environmental monitoring [8], surveillance [9], to name a few. In those applications, mobile robots are assumed to be simple, cheap, and disposable [10]. Toward deploying real mobile robots into those task environments, one of the technical challenges is to develop robot platforms at a reasonable cost. Specifically, sensing systems used in the platforms are essential in performing those tasks, because they play a role in detecting the presence of objects including neighboring robots, and measuring their relative positions. Unfortunately, the sensing systems are still high-priced devices and relatively large in size as compared with the platforms.

In most applications, mobile robots need to be able to observe their surroundings in all directions simultaneously. One of the most common options for 360-degree observation capability is to place an adequate number of sensors (closely spaced) at equal intervals around the circumference of the robot. Due to technical difficulties, such as the number of sensors required, interference, and cost, they would be hard to install uniformly. Another option is to develop a sensor capable of 360-degree rotation. This is inspired by biological evidence of what happens during the foraging behavior of echolocating bats [11]. Surprisingly, echolocating bats can control frequency and bandwidth of their signals. As illustrated in Fig. 1, when searching for prey, bats emit sound pulses in a regular pattern in all directions. After detecting the presence of prey, the pulse repetition rate increases in that direction to get accurate prey position. It should be noted that a proper implementation of bat-like sensing systems can be considered very cost-effective for robot swarm applications.

Fig. 1. Echolocation and pursuit of prey by bats

An important issue is how to coordinate a large number of robots without using costly hardware solutions. The use of high accuracy sensors helps ensure accurate distance and position measurements, but can become costly. For instance, we have spent about USD 50 fabricating one set of proximity sensor prototype with 360-degree observation capability. On the other hand, one of the most widely used laser sensors (Hokuyo Ltd.'s URG-04LX) with 240 degree range is 24 times more expensive than our prototype. Along this line, we developed a low-cost position detection prototype having a sensing angle of 360 degrees [12]. To increase the practical applicability of the sensor prototype in real environments containing a number of robots and obstacles, we need to develop an accurate, efficient multi-functional observation and detection algorithm.

The main purpose of this paper is to present 1) new prototype *dual rotating infrared* (DRIr) sensors for mobile robot swarms, 2) operation functions controlling observation motions by DRIr sensors, and 3) an observation algorithm enabling individual robots equipped with DRIr sensors to estimate the reliable center coordinates of other robots. First, we mechanically design DRIr sensor to give the robot a greater range of visibility. As relative location sensors for mobile robot swarms, we also consider the following design aspects: low cost, compactness, and easy integration. This paper provides a detailed presentation on how to build DRIr sensor prototype. Secondly, what is important from the practical point of view

is to realize several kinds of observing operations of each robot using DRIr sensors in an efficient way. From biological evidence, three types of operation functions are proposed to control rotation speed, intervals, and ranges of DRIr sensors. Specifically, when adjusting rotation ranges of DRIr sensors, robots determine their own sensing coverage area, allowing them to perform another task such as tracking a moving target. Further details on operation functions are described later in this paper. Thirdly, toward deployment of real mobile robots, it is also important to obtain reliable locations of neighboring robots and obstacles. For that purpose, an observation algorithm is proposed, which enables each robot to distinguish between other robots and obstacles, and then to obtain the reliable center coordinates of the robots. We explain how to implement the observation algorithm based on DRIr sensors. Finally, we performed experiments to demonstrate swarm deployment applications by commercial robots, where DRIr sensors allow them to obtain effective relative position sensing.

The rest of this paper is organized as follows. Section II gives a brief description of location-sensors used in mobile robots. Section III presents mechanical design, fabrication, integration of DRIr sensors, and preliminary results for the design concept of DRIr sensors. Section IV and Section V describe operation functions and the observation algorithm, respectively. Section VI illustrates experimental results and discusses our future directions. Section VII explains our conclusions.

II. Background: Comparison of Location-Sensing Systems

Location-sensing systems used in mobile robot platforms can be broadly classified into absolute and relative sensors, according to whether obtained location data is based on a fixed global reference or the local coordinates of a robot. To begin, the absolute location sensors include *global positioning system* (GPS) [13]-[15] using at least three satellites, and a central monitoring system such as an external camera [18]-[20]. Robots with GPS receivers can obtain their own 3-D location plus time information. With electronic advances, the receiver has been getting smaller. GPSs do not function indoors, because it is difficult to deal with signal blockage. Even though indoor signals are corrupted multi-path and severely attenuated, the recent indoor GPS runs satisfactorily [16][17]. If swarms of mobile robots containing GPS receivers are organized, this entails heavy outlays. The location data of other robots should be continuously updated through a different communication channel. When utilizing a central monitoring system, the expense for a mobile robot platform can be reduced. Similarly, robots might be burdened with continuous communications. The system requires a great deal of money to prevent blind spots.

Next, the relative location sensors include cameras [21]-[24], *received signal strength indicator* (RSSI) measurement systems [25]-[28], and proximity sensors [30]-[36]. First, a camera mounted on a robot takes a snapshot of its surroundings. Then, meaningful information is extracted from the snapshot through a series of computations. From the continuous process, the robot can recognize the presence of objects including neighboring robots. Although the camera can provide much information in only one snapshot, complicated computation algorithms and fast computing aids are needed. Moreover, the camera is very sensitive to illumination changes. When multiple robots equipped with cameras are deployed, this may be costly. To identify other robots, color bars [23] or helmets [24] indicating their identification numbers are additionally installed.

Secondly, RSSI measurement systems are employed in wireless environments based on wireless networking of the IEEE 802.11 protocol family [25][26] or *radio frequency identification* (RFID) [27]-[28]. Their usage makes additional information available to identify a specific robot without extra equipment. Moreover, RSSI measurement systems are not affected by any obstacles. Despite these advantages, the RSSI measurement needs other hardware devices, such as reader and antenna, separately. Due to low accuracy, it is difficult to deploy large-scale robot swarms using RSSI measurement systems. Differently from wireless environments, a similar technique using infrared arrays has been reported [29]. Its distinctive features are low-cost, very small size, and very fast update rate and communication. However, it is susceptible to interference from external signals, and has more restricted line-of-sight.

Thirdly, the proximity sensors are further classified into *laser range finder* (LRF) [30]-[32], ultrasonic sensor (for simplicity, sonar afterward) [33][34], and *infrared sensor* (Ir) [12][35][36]. The features of LRF are higher speed, accuracy, and resolution than sonar and Ir. LRF has generally been used in various applications of mobile robots, but the installation of LRF is too expensive. Compared with LRF, sonar and Ir are small and low cost. Accordingly, these merits can be directly connected with the swarm organization of lager numbers of mobile robots. Sonar based on time-of-flight distance measurement has a longer range than Ir, but is easily affected by the hardness of objects, (resulting in reflection and refraction). Ir based on parallax distance measurement can be cheaper and smaller than sonar, but is easily affected by the color of objects. Irs have less mutual interference between them. Recently, multi-sensor fusion techniques such as camera plus laser photo detector [37] and RSSI measurement based on sonar [38] have been introduced to make the most of mutual strengths.

III. Proximity Sensor Prototype Development

A. Proximity Sensor Prototype Configuration

Fig. 2 illustrates the configuration and the control schematic of the proposed proximity sensor prototype. The prototype largely consists of DRIr sensor and DRIr controller. To begin, DRIr sensor has two MiniStudio MiniS RB90 servo motors and one Sharp GP2Y0A02YK infrared sensor (Ir). Each servo motor is independently controlled by its controller. One servo motor rotates up to 180 degrees, thus two identical motors can sweep a full 360 degrees. As illustrated in Fig. 3, the base motor enables Ir to be directed toward a specific direction,

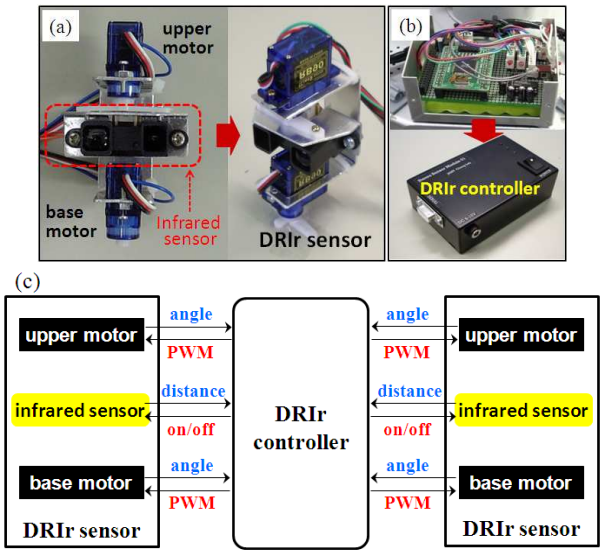

Fig. 2. Configuration and control architecture of the proximity sensor prototype ((a) DRIr sensor, (b) DRIr controller, (c) control architecture schematic)

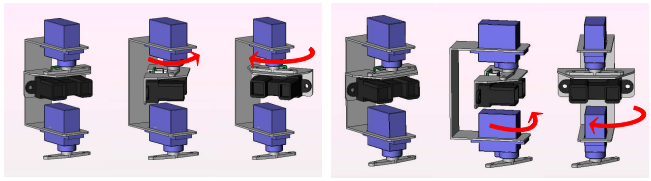

(a) rotation of the upper motor (b) rotation of the base motor

Fig. 3. Combined motions of sensor rotation in DRIr sensor

while the upper motor can rotate 180 degrees with respect to the direction of the base motor. By the combination of the base and upper motors, infrared rays can be emitted in a wide variety of directions. Further details on the combined motions are described in Section IV.

Next, in DRIr controller, the Atmel ATmega128 microcontroller is used to control each motor rotating Ir, and to feed the measured data to an outside component through an external communication channel (i.e., RS-232c). The controller forwards two-channel control signals to DRIr sensor. One signal controls the rotation angle of each motor by *pulse width modulation* (PWM). The other signal is used for on-off control of Ir. Moreover, the analog output voltage representing the distance to the detecting surface, where the voltage level decreases with increasing distance in a unimodal fashion from 12 *cm* to 160 *cm* [12], is fed to the controller and converted to 10-bit digital values. Finally, the detailed specifications of the proposed prototype are summarized in Table I.

B. Mobile Robot Integration

Our customized mobile robot is set to organize a swarm of mobile robots equipped with DRIr sensors. The mobile robot largely consists of three parts: MobileRobots Pioneer 3-DX as a mobile robot platform, a pair of DRIr sensors, and their main controller.

First, as shown in Fig. 4-(a), DRIr sensors mounted on the front and rear edges of the robot allow it to observe

TABLE I
SPECIFICATIONS OF DRIR SENSOR PROTOTYPE

Size	• DRIr sensor: 5.5×9.5×1.8 mm • DRIr controller: 10×6.5×3.5 mm
Weight	• DRIr sensor: 0.05 kg • DRIr controller: 0.12 kg
Speed	• max. angle velocity: 154 deg/sec • min. angle velocity: 14.9 deg/sec
Other	• power: DC 6 $\sim$ 15 V • external communication: RS-232c

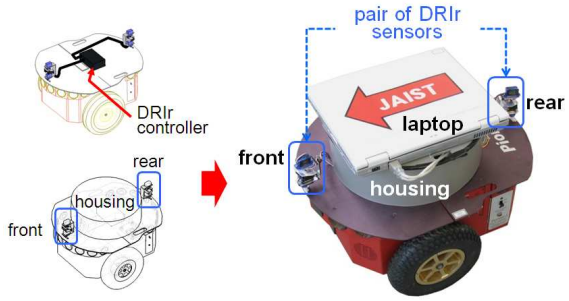

(a) mobile robot integration

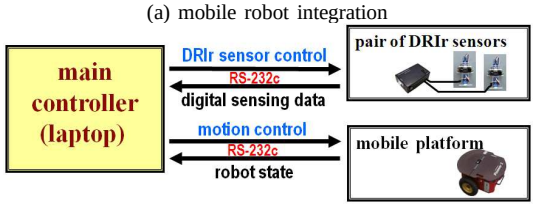

(b) overall control schematic

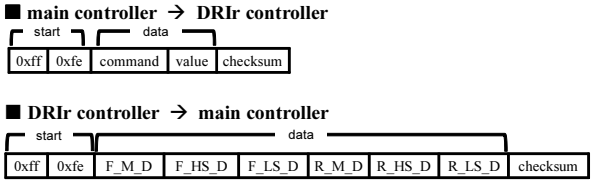

(c) two kinds of communication packets

Fig. 4. Integration of the mobile robot equipped with DRIr sensors

other robots in the forward and reverse directions simultaneously. By a pair of DRIr sensors, the robot can be provided with a sensing range up to 320 *cm*. Secondly, a laptop PC running Microsoft's Windows XP is used as the main controller, and is placed on top of the robot. Fig. 4-(b) shows the control schematic of the integrated overall mobile robot. The main controller is linked to DRIr controller and to the robot controller through RS-232c. Inputs to the main controller include the digitalized measurement data and the robot state. The main controller forwards control commands to DRIr controller and the robot controller. Fig. 4-(c) illustrates two kinds of communication packets between the main controller and DRIr controller. In particular, DRIr controller converts various operation commands from the main controller into PWM controlling the rotation motions. Details on these commands are further described in Section IV. Thirdly, the circular housing is designed for the cradle of the laptop and the container of DRIr controller. The border of the housing represents the surface geometry whose center point is easy to detect irrespective of the robot's heading. Specifically, the

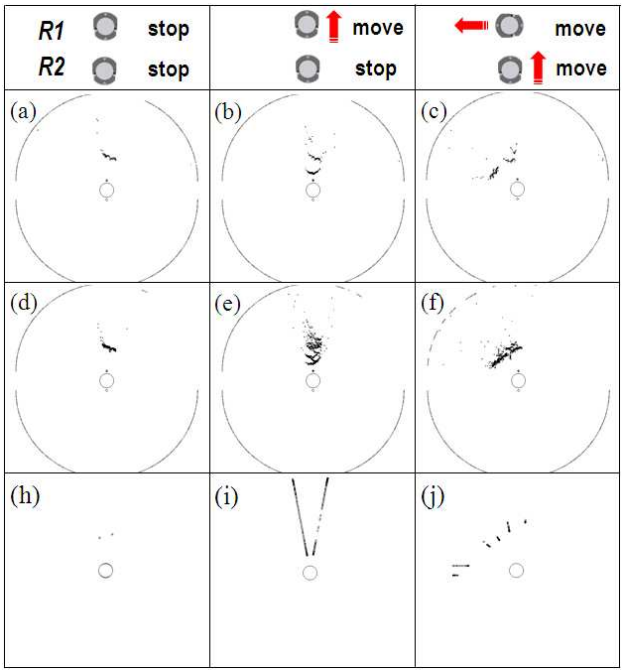

Fig. 5. Observation results by the *R2* robot according to three test conditions

housing's center coincides with the origin coordinates of the robot.

C. Preliminary Test Results

To examine observation effectiveness by the rotation of DRIr sensor prototype, we performed preliminary tests as shown in Fig. 5. Here, the robot *R2* observes the other robot *R1*; either of them may stop or move with uniform velocity. Figs. 5-(a) through (c), (d) through (f), and (h) through (j) show the observation results by *R2* when the prototype mounted on the front edge of *R2* rotates 240 degrees, the prototype rotates an assigned range while following the moving direction of *R1*, and the eight fixed prototypes are mounted on the front edge of *R2* at intervals of 30 degrees, respectively. The following three motion cases were considered: 1) *R1* and *R2* were stationary in Figs. 5-(a), (d), and (h), 2) *R1* moved away from *R2* in Figs. 5-(b), (e), and (i), and 3) *R1* and *R2* moved away at right angles or perpendicularly from each other in Figs. 5-(c), (f), and (j). From the results, we were convinced that the prototype rotation can provide real robots with much clearer and better organized location information than the fixed prototypes. More specifically, results of the assigned range rotation provide a fairly dense pattern of data, which can be effective in tracking a continuously moving robot. As shown in Fig. 5-(h), *R2* could obtain only two data point. Also note that *R2* roughly recognizes the movement direction of *R1* in Fig. 5-(j), but it is impossible to compute center coordinates of *R1* due to insufficient data. To pursue sufficient data, DRIr sensor prototype was developed with 360-degree observation capability, as the basic function, and with a particular emphasis on variable scanning range and speed, as extended functions.

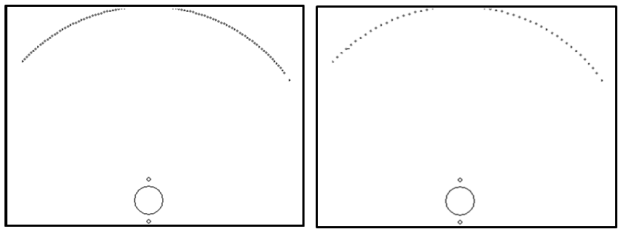

(a) fine rotation (b) coarse rotation

Fig. 6. Observation results according to the fine and coarse rotations

IV. Operation Functions of DRIr Sensors

Designed operation functions controlling the observation motions of DRIr sensor are composed of rotation speed, rotation interval, and rotation range functions. As shown in Table I, first, the rotation speed can be controlled in the range from 14.9 deg/sec to 154 deg/sec. Secondly, as the incremental angle of rotation can be adjusted, the angular resolution can be controlled accordingly. Here, the incremental angle of rotation is controlled by the fine and coarse rotation commands, enabling the servo motor to rotate a certain amount of degrees at one or two degree interval. Then Ir emits an infrared ray at each one or two degree interval. Fig. 6 shows the observation results of DRIr sensor controlled by the fine and coarse rotation commands, respectively. As expected, the fine rotation command offers higher spatial resolution for better characterization of the detected object. Meanwhile, the robot can observe the same range more quickly using the coarse rotation command. Now, we can implement two methods to control the observation frequency by adjusting either the speed or incremental angle of rotation.

Next, the observation bandwidth can be controlled through changing the rotation range in order to effectively implement the scanning and tracking functions, respectively. Fig. 7 illustrates the conceptual definition and the combined motion of two servo motors. For the scanning function, the front DRIr sensor scans from -120 degrees to 120 degrees in azimuth with respect to the heading of the robot, as illustrated in Fig. 7-(a). Here, the base motor rotates 180 degrees, and the upper motor adds another 60 degrees. The remaining 120 degree range cannot be observed, since the line-of-sight path is blocked by the housing, but is covered by the rear DRIr sensor that scans the same range in the opposite direction. Therefore, a pair of DRIr sensors can cover a full 360 degrees. The scanning function may be useful in checking the presence of other robots. On the other hand, for the tracking function, after the base motor turns toward a target, the upper motor rotates a certain limited amount of range on each side of the direction of the base motor, as illustrated in Fig. 7-(b). Thus, the tracking function is basically designed to follow as closely as possible a moving robot. By changing the rotation range, it becomes possible to control the observation bandwidth. A proper combination of desired observation frequency and bandwidth settings can be obtained depending on the purpose and circumstances.

In Table II, an experimental comparison on the performance of Hokuyo Ltd's URG-04LX and DRIr sensor is summarized.

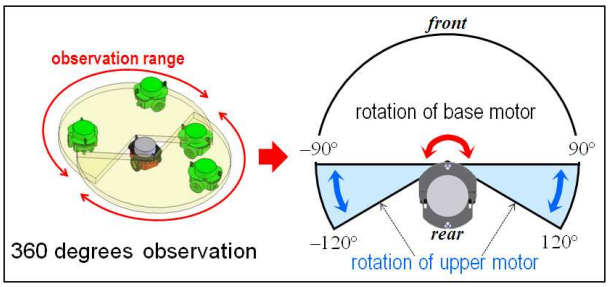

(a) scanning function

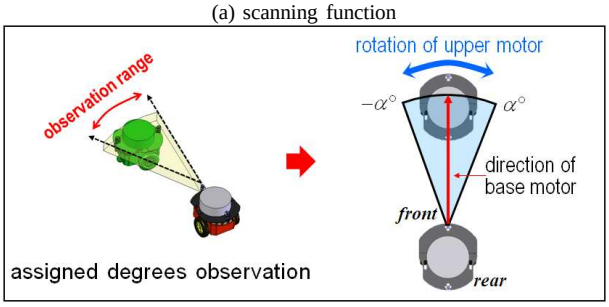

(b) tracking function

Fig. 7. Illustration of two observation bandwidth functions enabling a robot equipped with DRIr sensors to control rotation degrees

TABLE II
COMPARISON BETWEEN URG-04LX AND DRIR SENSOR

	URG-04LX (LFR)	DRIr sensor
Price (USD)	1200	50
Observation Range (degree)	240 (*fixed*)	$\leq$ max. 360 (*adjustable*)
Frame Rate (Hz)	10	min. 0.85 $\leq$ (*adjustable*)
Angular Interval (degree)	0.36	min. 1 $\leq$ (*adjustable*)
Accuracy (mm) (objects 1 m away)	$\pm$ 7	$\pm$ 26

Note that the frame rate in DRIr sensor varies according to the range and speed of scanning or tracking. Moreover, the observation resolution depends on the incremental angle of rotation.

V. OBSERVATION ALGORITHM AND ITS EVALUATION

Before explaining the algorithm, notations frequently used in its description are defined. We consider a robot r_i with local coordinates $\vec{l}_{x,i}$ and $\vec{l}_{y,i}$ as illustrated in Fig. 8. Here, $\vec{l}_{x,i}$ defines the vertical axis of r_i's coordinates as its heading direction, and $\vec{l}_{y,i}$ denotes the horizontal axis by rotating the vertical axis 90 degrees counterclockwise. Moreover, the center position of a robot r_i is defined as p_i with respect to its local coordinates. The distance between the robot r_i's position p_i and another robot r_j's position p_j is denoted as $dist(p_i, p_j)$.

The proposed observation algorithm aims at distinguishing between homogeneous robots and obstacles within the coverage range of DRIr sensors, and obtaining reliable robot positions. The algorithm is described through the three steps detailed below. First, the measurement step constructs two one-dimensional arrays in the memory of r_i as shown in Fig. 8-(a). Here, the dimension of each array can be automatically adjusted according to rotation intervals and ranges. When r_i scans its environment using DRIr sensors at the assigned intervals, the distances to the surfaces of objects including robots are recorded in the corresponding cell of the first array. At the same time, the motor angle is recorded in the second array, so that the distance array corresponds to the motor angle array. Next, r_i checks its distance array cells that contain a non-zero value (from the lower bound d_{min} to the upper bound d_{max}) and reads the corresponding angle array cells. As shown in Fig. 8-(b), the distance and angle data are converted to x-y coordinates with respect to $\vec{l}_{x,i}$ and $\vec{l}_{y,i}$.

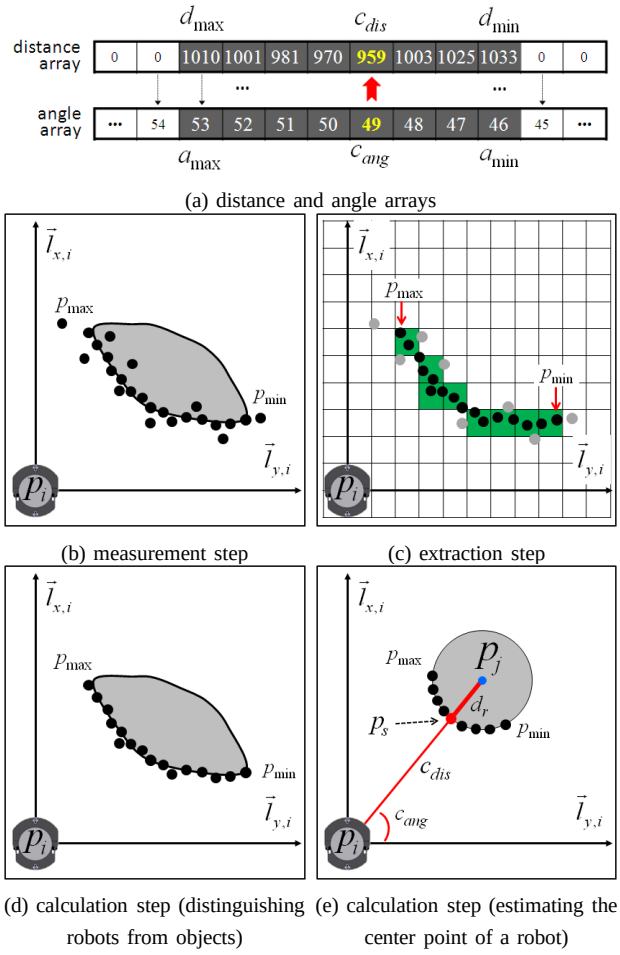

(a) distance and angle arrays

(b) measurement step (c) extraction step

(d) calculation step (distinguishing robots from objects) (e) calculation step (estimating the center point of a robot)

Fig. 8. Illustration of the observation algorithm

Secondly, the extraction step extracts more reliable data from the measurement data with respect to a reference. For the purpose, a 80 $\times$ 80 2-D grid with 4 cm $\times$ 4 cm unit cells is built, as shown in Fig. 8-(c). The converted coordinates in the measurement step are simultaneously stored in the corresponding cell of the grid as an integer intensity value. Once the rotation of the assigned range is completed, the Sobel edge detection algorithm [40] is employed to improve the original surface detection data.

Thirdly, the calculation step differentiates robots from objects, and then identifies the positions of the robots. The cells estimated through edge detection are collected, and the distance and angle arrays are re-arranged according to the

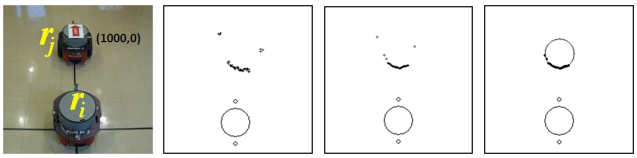

(a) test scene (b) measurement (c) extraction (d) calculation

Fig. 9. Observation process of the neighbor robot r_j by the robot r_i

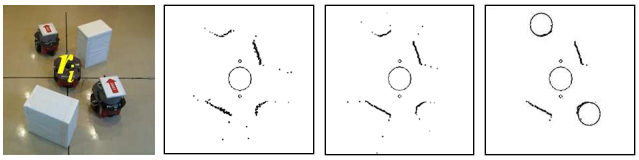

(a) test scene (b) measurement (c) extraction (d) calculation

Fig. 10. Observation process of multiple robots and obstacles by the robot r_i

corresponding grid cells. Then, r_i newly defines the distance arrays from d_{min} to d_{max}. Similarly, it defines the angle arrays from a_{min} to a_{max} corresponding to the distance arrays. Here, the two geometric feature points p_{min} and p_{max} are specified using d_{min} and a_{min} and d_{max} and a_{max}, respectively. Next, r_i computes $dist(p_{min}, p_{max})$ and checks whether $dist(p_{min}, p_{max})$ is longer than the housing diameter. If $dist(p_{min}, p_{max})$ exceeds the diameter, the collected cells are considered to be obstacles, as shown in Fig. 8-(d). Otherwise, these cells are considered to be robots. Note that, to identify the robot shape, there are two further conditions to be satisfied. Details on the conditions are found in [12]. Through the above process, if robots are recognized, a center point p_j can be obtained by adding c_{dis} to the housing's radius d_r (see Fig. 8-(e)). Note that the observation algorithm requires robots to be initially positioned a minimum distance of 150 *mm* away from DRIr sensors, with a clear line of sight.

To demonstrate the verification of the observation algorithm, we performed two kinds of tests. In the first test, seen in Fig. 9-(a), r_i observes its neighbor r_j located 100 cm away. Figs. 9-(b), (c), and (d) show the data processing results obtained through the measurement, extraction, and calculation steps, respectively. Compared with Fig. 9-(b), Fig. 9-(c) shows enhanced surface detection by eliminating blurred and distorted edges. Finally, r_i could recognize r_j as shown in Fig. 9-(d). Next, Fig. 10 presents the observation results with two neighboring robots and obstacles. Similarly, compared with Fig. 10-(b), Fig. 10-(c) shows enhanced surface detection. Moreover, as shown in 10-(d), r_i could distinguish between robots and obstacles. From the results, the proposed algorithm using DRIr sensors could provide robots with enhanced observation capabilities.

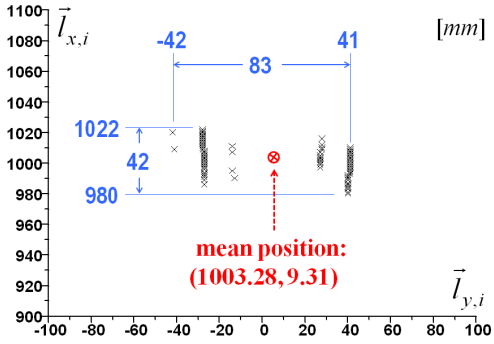

(a) r_j's center point in the measurement step

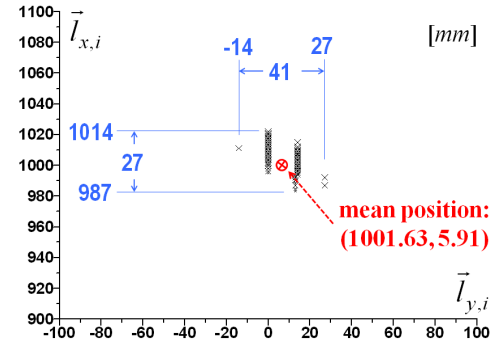

(b) r_j's center point in the calculation step

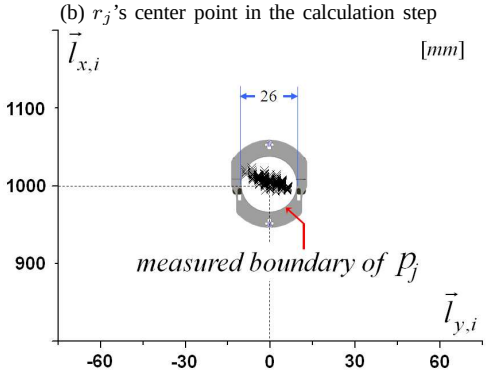

(c) average boundary of r_j's estimated center point

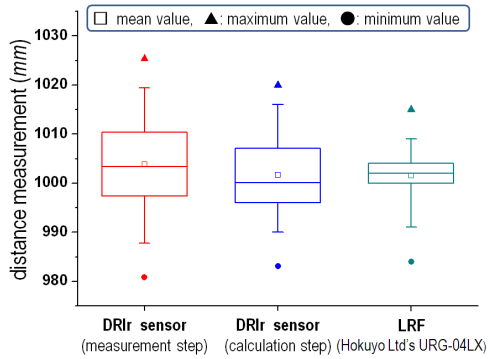

(d) comparison between DRIr sensor and LRF

Fig. 11. Estimation of r_j's center point in Fig. 9-(a)

VI. Experimental Results and Discussion

This section presents the experimental results for the observation capability of DRIr sensors, their operation controls, and formation control applications of mobile robot swarms. In our experiments, we use homogenous robots, each of which is equipped with a pair of DRIr sensors, but unable to identify each other. DRIr sensors emit an infrared ray every one degree.

First, analytic experiments were executed to evaluate the effectiveness of the observation algorithm, with the results of 300 trials in the condition of Fig. 9-(a). Figs. 11-(a) and (b) show the estimation results of r_j's center point through each step of the process. Compared with Fig. 11-(a), the proposed algorithm enables the estimates to be gathered around the

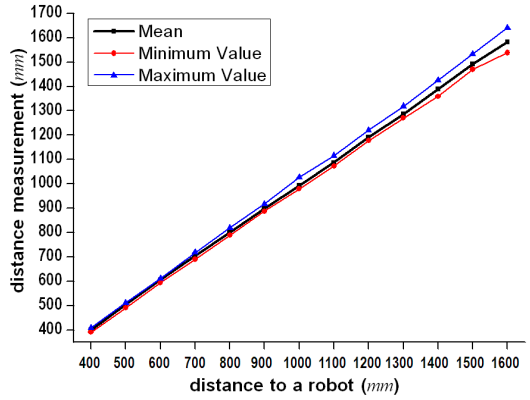

Fig. 12. Statistical analysis results of 300 trials over distances to r_j measured at intervals of 100 mm

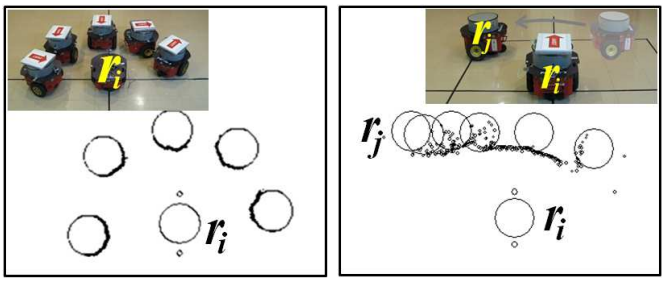

(a) (b)

Fig. 13. Observation results for the scanning and the tracking functions ((a) observing five neighboring robots using the scanning function, (b) observing a neighboring robot moving with non-uniform velocity using the tracking function)

mean position in Fig. 11-(b). From the result, it can be confirmed that the algorithm is effective in enhancing its accuracy. Fig. 11-(c) shows that the average error in estimating the center point p_j of r_j resides within a 2.6 cm radius circle. In other words, this numerical value indicates the average distance error rate is $\pm$ 2.6% when the target robot is apart 1000 mm distant from r_i. In similar fashion to Fig. 9-(a), Fig. 11-(d) shows the results of statistical analysis of distances to r_j estimated by DRIr sensor and Hokuyo's URG laser scanner (LRF). Here, the squares, triangles, and circles indicate the mean value, maximum value and minimum value, respectively. The whiskers represent the range of 5% to 95% confidence intervals, and the boxes indicate distributions of measured data in the range of 25% to 75%. LRF outperforms DRIr sensor in terms of accuracy, but DRIr sensor also shows reasonably good accuracy. Fig. 12 presents the statistical analysis results of 300 trials over distances to r_j measured at intervals of 100 mm in the range of 400 mm through 1600 mm. Although the measurement accuracy is degraded at a long distance (i.e., far away from 1100 mm), from the results that we have seen so far, DRIr sensor observation capability can be considered quite satisfactory for practical use.

Secondly, to differentiate between the scanning and tracking observations by DRIr sensors, two kinds of tests were performed. Above all, Fig. 13 presents observation results obtained by the scanning and tracking functions, respectively. As shown in Fig. 13-(a), the robot r_i simultaneously observes

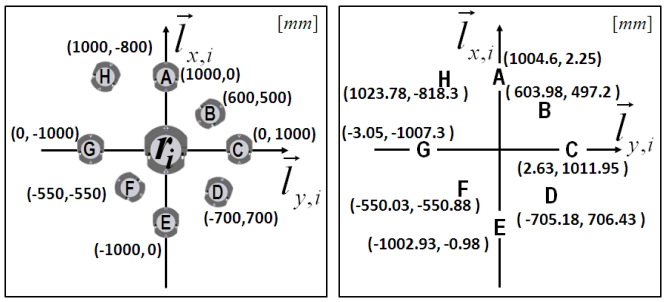

(a) eight deliberately-positioned neighboring robots (b) average center points of the neighboring robots

Fig. 14. Observation results for deliberately positioned 8 neighboring robots

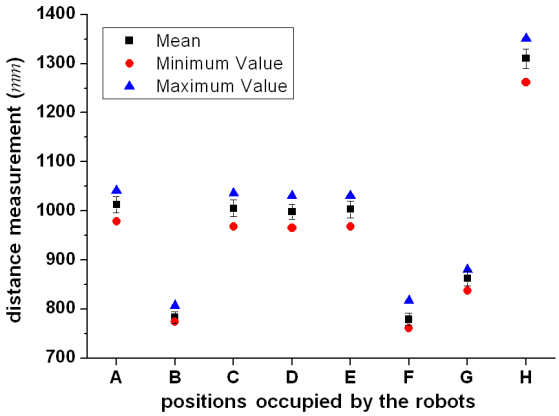

Fig. 15. Statistical analysis of distance measurements in Fig. 14

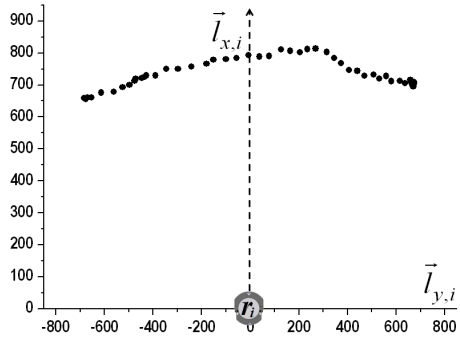

Fig. 16. Estimation of r_j's center points in Fig. 13-(b)

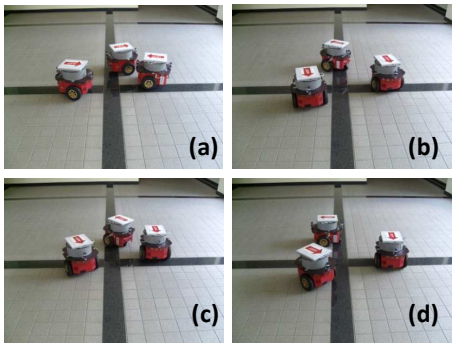

Fig. 17. Geometric local interaction forming an equilateral triangle by 3 mobile robots

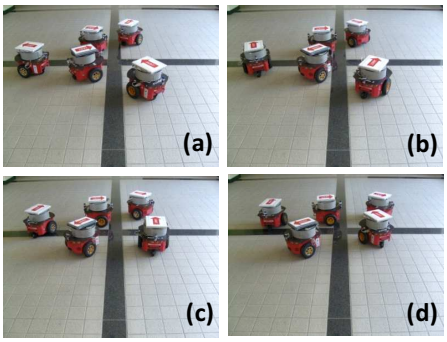

Fig. 18. Self-configuration by 5 mobile robots in a free open space

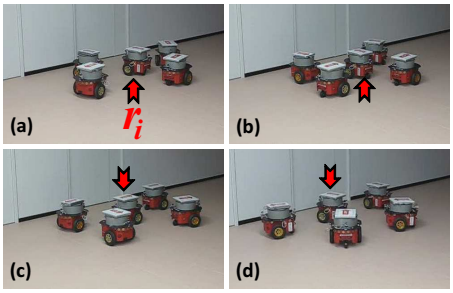

Fig. 19. Self-configuration conforming to a flat border

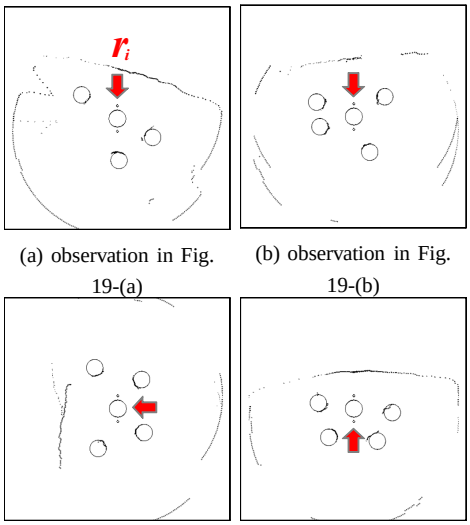

(a) observation in Fig. 19-(a) (b) observation in Fig. 19-(b)

(c) observation in Fig. 19-(c) (d) observation in Fig. 19-(d)

Fig. 20. Observation results during self-configuration in Fig. 19

five neighboring robots using the scanning function. The result clearly shows that DRIr sensors can cover a full 360 degrees. Fig. 13-(b) presents the consecutive observation results for a neighboring robot r_j moving with non-uniform velocity, using the tracking function. Note that the tracking function works satisfactorily, even if the velocity of r_j fluctuates up and down rapidly.

Next, experiments were performed to provide quantitative analysis of the scanning and tracking observation by DRIr sensors. As shown in Fig. 14-(a), eight neighboring robots are deliberately positioned around r_i. Figs. 14-(b) and 15 show the scanning observation results of 300 trials when robots

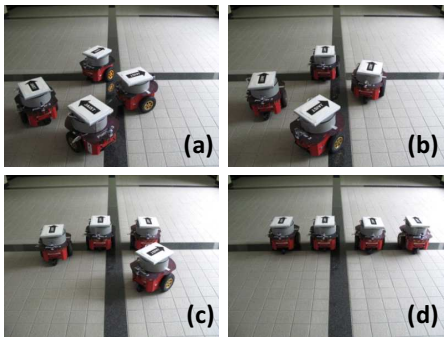

Fig. 21. Experimental results for one row pattern generation

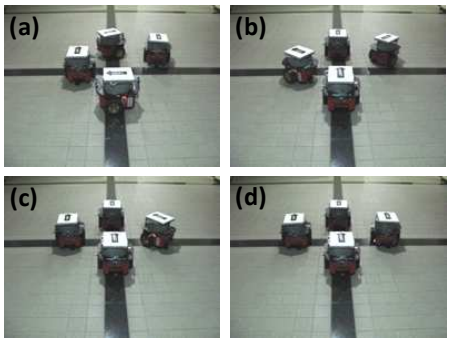

Fig. 22. Experimental results for a diamond pattern generation

are observed simultaneously through a pair of DRIr sensors. Specifically, Fig. 15 shows the results of statistical analysis of estimated distances between the robots. Here, the square, triangle, and circle indicate the mean value, maximum value and minimum value, respectively. The whiskers represent the range of 5% to 95% confidence intervals. Fig. 16 presents the observation result for a moving robot r_j in the same fashion as Fig. 13-(b). Similarly, Fig. 16 shows that r_i could compute the center points of r_j moving within the velocity. From the results, DRIr sensor observation capability can be considered quite satisfactory for practical use.

Thirdly, to verify the effectiveness and feasibility of DRIr sensors in swarm deployment applications, we demonstrated three kinds of experiments: 1) self-configuration [5][39] that enables robots to configure themselves into an area while forming equilateral triangle lattices, 2) pattern generation [3] to create geometric shapes where the robots track their target robot according to the desired shape, and 3) flocking [7] to make a coordinated group movement. In these experiments, robots are initially located at arbitrary positions with different heading directions. They attempt to form a coordinated configuration starting from no *a priori* coordinate agreement, moving with a linear velocity of 150 *mm/s* and an angular velocity of 100 *deg/s*. The desired inter-robot distance d_u in formation patterns is 80 cm. At any time, the deployment algorithms enable each robot to compute its position at the next time step based on the observation algorithm. These iterative activations are controlled by the main controller.

As shown from Fig. 17 through Fig. 19, self-configuration experiments were performed. Figs. 17 and 18 show the snapshots of the self-configuration process in an open space.

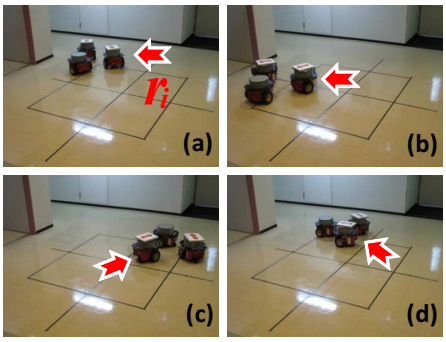

Fig. 23. Tracking a target moving along a square trajectory

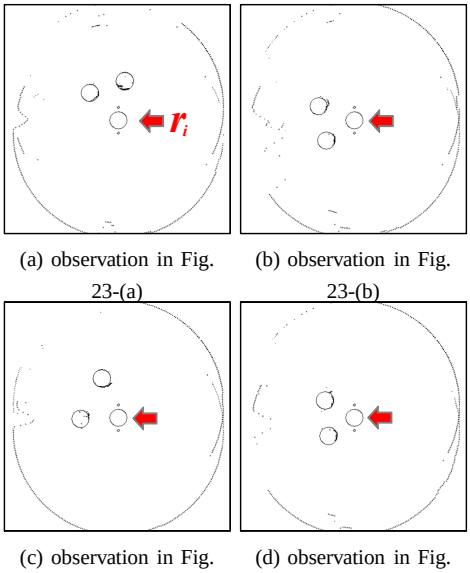

(a) observation in Fig. 23-(a)

(b) observation in Fig. 23-(b)

(c) observation in Fig. 23-(c)

(d) observation in Fig. 23-(d)

Fig. 24. Observation result of r_i during the target tracking in Fig. 23

Three-robot and five-robot swarms could generate equilateral triangles with d_u between neighboring robots. Fig. 19 shows snapshots of the self-configuration process in a geographically-constrained space. In Fig. 20, the output of the robot r_i's observation result at each corresponding process step in Fig. 19 is shown. Moreover, the area border (wall) was also detected by DRIr sensors. Next, neighbor-referenced pattern generation experiments were performed. Figs. 21 and 22 show how to generate one row and diamond patterns by the four robots, respectively. Robots follow their neighbor robot by keeping d_u and a predetermined angle according to the desired shape until the neighbor stops moving. In Fig. 23, three robots form an equilateral triangle while a target robot is teleoperated by a human operator. Fig. 24 displays the results of observation of other robots performed by r_i. After starting from the initial random distribution in Fig. 23-(a), two robots successfully tracked the target with which they form an equilateral triangle. From these results, we have verified that robots equipped with DRIr sensors could self-configure themselves into an area, generate geometric patterns, and navigate while maintaining equilateral triangles under our laboratory conditions.

We believe that the proposed DRIr sensors will work well under real world conditions, but several issues remain to be solved. First of all, to distinguish between other robots and various objects quickly and accurately, it can be advantageous to fuse DRIr sensors and RFID systems for extending swarm applications in obstacle-cluttered environments. It is also required to develop recognition algorithms suited for different types of robots. Specifically, to provide the robots with reliable shape recognition capability for various objects, we are currently working on developing a more sophisticated proximity sensor prototype capable of translating and rotating observation motions.

VII. Conclusions

In this paper, we addressed practical design and hardware implementation of the DRIr proximity sensors for mobile robot swarms. Features include low cost, high reliability, and easy integratability into commercial mobile robots. To mainly provide robots with full 360-degree azimuth scanning and controllable range-tracking capabilities, the operation functions controlling the observation motions were realized. Based on the proposed observation algorithm, each robot could obtain relative positioning information, as well as distinguish neighboring robots from obstacles in an unknown environment. The hardware prototype and control schemes were implemented employing commercial mobile robot platforms. Extensive real robot experiments were performed to show the validity of the proposed features. Specifically, we successfully demonstrated three deployment applications of a swarm of mobile robots. Finally, DRIr sensors can be cost-effectively applied to mobile robotic sensor networks for unmanned surveillance missions.

References

[1] H. Choset, "Coverage for robotics - a survey of recent results," *Annals of Mathematics and Artificial Intelligence*, vol.31, no.1-4, 2001, pp.113-126.

[2] Y. Ikemoto, Y. Hasegawa, T. Fukuda, and K. Matsuda, "Graduated spatial pattern formation of robot group," *Information Science*, vol.171, no.4, 2005, pp.431-445.

[3] G. Lee and N. Y. Chong, "Decentralized formation control for small-scale robot teams with anonymity," *Mechatronics*, vol.19, no.1, 2009, pp.85-105.

[4] B. Shucker, T. D. Murphey, and J. K. Bennett, "Convergence-preserving switching for topology-dependent decentralized systems," *IEEE Trans. Robotics*, vol.24, no.6, 2008, pp.1405-1415.

[5] G. Lee and N. Y. Chong, "A geometric approach to deploying robot swarms," *Annals of Mathematics and Artificial Intelligence*, vol.52, no.2-4, 2009, pp.257-280.

[6] J. Ghommam and F. Mnif, "Coordinated path-following control for a group of underactuated surface vessels," *IEEE Trans. Industrial Electronics*, vol.56, no.10, 2009, pp.3951-3963.

[7] G. Lee and N. Y. Chong, "Adaptive flocking of robot swarms: algorithms and properties," *IEICE Trans. Communications*, vol.E91-B, no.9, 2008, pp.2848-2855.

[8] C. A. Boano, N. Tsiftes, T. Voigt, J. Brown, and U. Roedig, "The impact of temperature on outdoor industrial sensornet applications," *IEEE Trans. Industrial Informatics*, vol.6, no.3, 2010, pp.451-459.

[9] S. Shin, T. Kwon, G.-Y. Jo, Y. Park, and H. Rhy, "An experimental study of hierarchical intrusion detection for wireless industrial sensor networks," *IEEE Trans. Industrial Informatics*, vol.6, no.4, 2010, pp.744-757.

[10] E. Sahin, "Swarm robotics: from sources of inspiration to domains of application," *8th Int. Conf. Simulation of Adaptive Behavior* (LNCS), vol.3342, 2005, pp.10-20.

[11] J. A. Simmons, M. B. Fenton, and M. J. O'Farrell, "Echolocation and pursuit of prey by bats," *Science*, vol.203, no.4375, 1979, pp.16-21.

[12] G. Lee, S. Yoon, N. Y. Chong, and H. I. Christensen, "Self-configuring Robot Swarms with Dual Rotating Infrared Sensors," *Proc. IEEE/RSJ Int. Conf. Intelligent Robots and Systems*, 2009, pp.4357-4362.

[13] K.-F. Ssu, C.-H. Ou, and H. Jiau, "Localization with mobile anchor points in wireless sensor networks," *IEEE Trans. Vehicular Technology*, vol.54, no.3, 2005, pp.1187.1197.

[14] A. Georgiev and P. K. Allen, "Localization methods for a mobile robot in urban environments," *IEEE Trans. Robotics*, vol.20, no.5, 2004, pp.851-864.

[15] S. Panzieri, F. Pascucci, and G. Ulivi, "An outdoor navigation system using GPS and inertial platform," *IEEE/ASME Trans. Mechatronics*, vol.7, no.2, 2002, pp.134-142.

[16] D. G. Seo and J. M. Lee, "Localization Algorithm for a mobile robot using iGS," *Proc. 17th World Congress The Int. Federation of Automatic Control*, 2008, pp.742-747.

[17] H. Niwa, K. Kodaka, Y. Sakamoto, M. Otake, S. Kawaguchi, K. Fujii, Y. Kanemori, and S. Sugano, "GPS-based indoor positioning system with multi-channel pseudolite," *Proc. IEEE Int. Conf. Robotics and Automation*, 2008, pp.905-910.

[18] T. Sasaki, D. Brscic, and H. Hashimoto, "Human-observation-based extraction of path patterns for mobile robot navigation," *IEEE Trans. Industrial Electronics*, vol.57, no.4, 2010, pp.1401-1410.

[19] J. Chen, D. Sun, J. Yang, and H. Chen, "Leader-follower formation control of multiple non-holonomic mobile robots incorporting a receding-horizon scheme," *The International Journal of Robotics Research*, vol.29, no.6, 2010, pp.727-747.

[20] D. Pizarro, M. Mazo, E. Santiso, M. Marron, D. Jimenez, S. Cobreces, and C. Losada, "Localization of mobile robots using odometry and an external vision sensor," *Sensors*, vol.10, no.4, 2010, pp.3655-3680.

[21] N. Moshtagh, N. Michael, A. Jadbabaie, and K. Daniilidis, "Vision-based, distributed control laws for motion coordination of nonholonomic robots," *IEEE Trans. Robotics*, vol.25, no.4, 2009, pp.851-860.

[22] A. E. Turgut, H. Celikkanat, F. Gokce, and E. Sahin, "Self-organized flocking with a mobile robot swarm," *Proc. 7th Int. Conf. Autonomous Agents and Multiagent Systems*, 2008, pp.39-46.

[23] L. Parker, B. Kannan, F. Tang, and M, Bailey, "Tightly-coupled navigation assistance in heterogeneous multi-robot teams," *Proc. IEEE/RSJ Int. Conf. Intelligent Robots and Systems*, 2004, pp.1016-1022.

[24] J. Fredslund and M. J. Mataric, "A general algorithm for robot formations using local sensing and minimal communication," *IEEE Trans. Robotics and Automation*, vol.18, no.5, 2002, pp.837-846.

[25] A. Koubaa, R. Severino, M. Alves, and E. Tovar, "Improving Quality-of-Service in Wireless Sensor Networks by Mitigating "Hidden-Node Collisions"," *IEEE Trans. Industrial Informatics*, vol.5, no.3, 2009, pp.299-313.

[26] J. Graefenstein and M. E. Bouzouraa, "Robust method for outdoor localization of a mobile robot using received signal strength in low power wireless networks," *Proc. IEEE Int. Conf. Robotics and Automation*, 2008, pp.33-38.

[27] S. Park and S. Hashimoto, "Autonomous mobile robot navigation using passive RFID in indoor environment," *IEEE Trans. Industrial Electronics*, vol.56, no.7, 2009, pp.2366-2373.

[28] M. Kim and N. Y. Chong, "RFID-based mobile robot guidance to a stationary target," *Mechatronics*, vol.17, no.4-5, 2007, pp.217-229.

[29] J. Pugh, X. Raemy, C. Favre, R. Falconi, and A. Martinoli, "A fast on-board relative positioning module for multi-robot systems," *IEEE/ASME Trans. Mechatronics*, vol.14, no.2, 2009, pp.151-162.

[30] R. Kurazume, Y. Noda, Y. Tobata, K. Lingemann, Y. Iwashita, and T. Hasegawa, "Laser-based geometric modeling using cooperative multiple mobile robots," *Proc. IEEE Int. Conf. Robotics and Automation*, 2009, pp.3200-3205.

[31] C. Ye, "Navigating a mobile robot by a traversability field histogram," *IEEE Trans. Systems, Man, and Cybernetics-Part B: Cybernetics*, vol.37, no.2, 2007, pp.361-372.

[32] H. Surmann, A. Nuchter, and J. Hertzberg, "An autonomous mobile robot with a 3D laser range finder for 3D exploration and digitalization of indoor environments," *Robotics and Autonomous Systems*, vol.45, no.3-4, 2003, pp.181-198.

[33] T.-H. S. Li, Y.-C. Yeh, J.-D. Wu, M.-Y. Hsiao, and C.-Y. Chen, "Multifunctional intelligent autonomous parking controllers for carlike mobile robots," *IEEE Trans. Industrial Electronics*, vol.57, no.5, 2010, pp.1687-1700.

[34] K. Lee and W. K. Chung, "Effective maximum likehood grid map with conflict evaluation filter using sonar sensors," *IEEE Trans. Robotics*, vol.25, no.4, 2009, pp.887-901.

[35] J. F. Roberts, T. S. Stirling, J.-C. Zufferey, and D. Floreano, "2.5D infrared range and bearing system for collective robotics," *Proc. IEEE/RSJ Int. Conf. Intelligent Robots and Systems*, 2009, pp.3659-3664.

[36] G. Benet, F. Blanes, J. E. Simo, and P. Perez, "Using infrared sensors for distance measurement in mobile robots," *Robotics and Autonomous Systems*, vol.40, no.4, 2002, pp.255-266.

[37] R. C. Luo and K. L. Su, "Multilevel multisensor-based intelligent recharging system for mobile robot," *IEEE Trans. Industrial Electronics*, vol.55, no.1, 2008, pp.270-279.

[38] F. Rivard, J. Bisson, F. Michaud, and D. Letourneau, "Ultrasonic relative positioning for multi-robot systems," *Proc. IEEE Int. Conf. Robotics and Automation*, 2008, pp.323-328.

[39] G. Lee and N. Y. Chong, "Self-configurable mobile robot swarms with hole repair capability," *IEEE/RSJ Int. Conf. Intelligent Robots and Systems*, 2008, pp.1403-1408.

[40] R. C. Gonzalez and R. E. Woods, *Digital image processing*, (2nd ed.) Prentice Hall, 2002.